Proteolytic Enzymes and Altered Glycosylation Modulate Dystroglycan Function in Carcinoma Cells

Jarnail Singh,[1] Yoko Itahana,[1] Selena Knight-Krajewski,[1] Motoi Kanagawa,[3] Kevin P. Campbell,[3] Mina J. Bissell,[2] and John Muschler[1]

[1]California Pacific Medical Center Research Institute, San Francisco, California; [2]Division of Life Sciences, Lawrence Berkeley National Laboratory, Berkeley, California; and [3]Department of Physiology and Biophysics, Howard Hughes Medical Institute, University of Iowa College of Medicine, Iowa City, Iowa

ABSTRACT

Alterations in the basement membrane receptor dystroglycan (DG) are evident in muscular dystrophies and carcinoma cells and characterized by a selective loss or modification of the extracellular α-DG subunit. Defects in posttranslational modifications of DG have been identified in some muscular dystrophies, but the underlying modifications in carcinoma cells have not yet been defined. We reveal here multiple posttranslational modifications that modulate the composition and function of DG in normal epithelial cells and carcinoma cells. We show that α-DG is shed from the cell surface of normal and tumorigenic epithelial cells through a proteolytic mechanism that does not require direct cleavage of either α- or β-DG. Shedding is dependent on metalloprotease activity and the proprotein convertase furin. Surprisingly, furin is also found to directly process α-DG as a proprotein substrate, changing the existing model of DG composition. We also show that the glycosylation of α-DG is altered in invasive carcinoma cells, and this modification causes complete loss of laminin binding properties. Together, these data elucidate several novel events regulating the functional composition of DG and reveal defects that arise during cancer progression, providing direction for efforts to restore this link with the basement membrane in carcinoma cells.

INTRODUCTION

Dystroglycan (DG) is an integral membrane receptor that links the extracellular matrix (ECM) to the cytoskeleton and mediates cell-ECM communications in a wide variety of cell types, including muscle, neural, and epithelial cells (1, 2). First identified by its association with dystrophin in muscle cells (3), DG has since been found to play diverse and important roles in cell function, including adhesion (4), sarcolemmal integrity (5), neurological development (6), basement membrane assembly (7), and epithelial polarization and morphogenesis (8–10), and also acts as a receptor for bacterial and viral infection (11, 12). Importantly, loss or alteration of DG function has been clearly implicated in several disease states from muscular dystrophies to neuronal disorders to cancer progression (9, 13, 14). Therefore, the factors regulating DG function in normal and diseased cells have become increasingly important to understand.

DG consists of two polypeptide subunits, α- and β-DG, that are synthesized from a single mRNA and subsequently cleaved to form the two subunits (see Fig. 1A). α-DG is retained at the cell surface by noncovalent association with β-DG and binds to ECM components such as laminin, agrin, and perlecan (1). β-DG spans the membrane and links to the cytoskeleton through its COOH-terminal cytoplasmic domain. α-DG consists of an NH$_2$-terminal and a COOH-terminal globular domain separated by an extended mucin-like region. Exten-

sive O-linked glycosylation in the middle domain mediates interaction with laminins and other ECM molecules (15, 16). The predicted protein molecular mass of the α-DG polypeptide is $\sim$75 kDa, yet the apparent molecular mass of α-DG varies from 120 to 200 kDa, reflecting extensive glycosylation. Complexity is evident in the posttranslational modifications of the α- and β-DG molecules, and these variations can impact receptor function (13). Altered glycosylation can eliminate binding of α-DG to ECM components and has already been implicated in diseases, including Fukuyama congenital muscular dystrophy and muscle-eye-brain disease (13, 16, 17). Another factor contributing to variations in DG composition is the apparent shedding of α-DG from the cell surface, detected in both normal and cancerous cells (18, 19).

Whereas some of the modifications in DG that contribute to muscular dystrophies have been elucidated (13, 17), the modifications in DG that arise in cancer cells remain obscure. Expression of wild-type DG cDNA in carcinoma cells did not restore detectable α-DG in most cases, implicating posttranslational modifications as the primary defect (9). The apparent ratio of α-DG/β-DG is highly variable in cancer cells, despite the fact that α- and β-DG are the translation products of a single gene, and points to a selective loss of the α-DG subunit at the cell surface (9, 20). However, these observations are complicated by the fact that the monoclonal antibodies used to detect the α-DG subunit in human cells (IIH6 and VIA4) depend on carbohydrate modifications for epitope binding (4). Reports using carcinoma cells and tissues have suggested that cleavage of the 43-kDa β-DG to a 31-kDa form results in loss of the NH$_2$-terminal portion of β-DG that tethers α-DG and correlates with loss of α-DG itself (20, 21). Another study, using a variety of cell types, demonstrated that β-DG was cleaved at the cell surface by a metalloprotease (MP), and these authors also concluded that loss of α-DG was a consequence of β-DG cleavage (22). However, neither study demonstrated that α-DG levels were indeed altered by inhibition of β-DG cleavage. Although cleavage of β-DG could be one cause for loss of α-DG, this alone does not appear to explain the widely variable ratio of detectable α-DG/β-DG (9).

Here we examine the posttranslational modifications regulating DG in nonmalignant breast epithelial cells and carcinoma cells. We establish that multiple independent cleavage events, involving MPs and furin, regulate the fate of both α- and β-DG and alter the levels of functional receptor on the cell surface. Furin is observed to directly cleave α-DG, removing the NH$_2$-terminal globular domain but preserving laminin binding function. These cleavage events occur in both functionally normal and tumorigenic epithelial cells. Last but not least, we reveal that, similar to observations in some muscular dystrophies, altered glycosylation of α-DG is the principle cause for the loss of DG function in invasive carcinoma cells.

MATERIALS AND METHODS

Chemicals. The IIH6 anti-α-DG antibody has been described previously (3). The anti-β-DG antibody (clone NCL-β-DG) was purchased from Novacastra Laboratories (Newcastle upon Tyne, United Kingdom), and anti-E-cadherin antibody (clone 36) was purchased from Transduction Laboratories
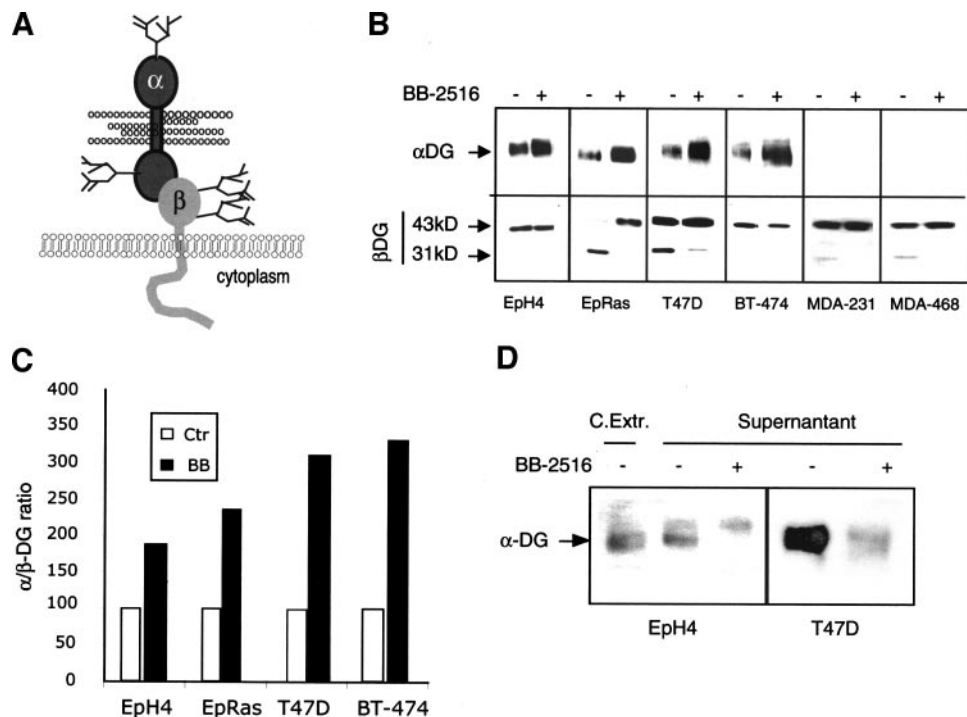
Fig. 1. MP activity induces loss of α-DG in normal mammary epithelial cells and breast tumor cell lines. *A*, structure of α- and β-DG. α-DG is a dumbbell-shaped molecule with an NH$_2$-terminal and a COOH-terminal globular domain, separated by a mucin-like domain. α-DG forms a noncovalent linkage with β-DG, which spans the plasma membrane and thereby links α-DG to the cytoskeleton. O-linked glycosylation is shown as a *chain of circles* of varying length, whereas N-linked glycosylation is shown as *branches*. *B*, immunoblot analysis of α- and β-DG levels in cell lines cultured in the presence or absence of the MP inhibitor BB-2516. Cells were cultured in serum-free medium for 2 days with or without BB-2516, and then total cellular proteins were extracted and subjected to immunoblot analysis of α-and β-DG. *C*, ratio of α-DG/β-DG levels from cell extracts in *B*. Intensities of individual bands were quantified, and the α-DG/β-DG ratio was calculated. The α-DG/β-DG ratio of untreated cells was set at 100%, and that of BB-2516-treated cells was calculated as the percentage increase from the control. *D*, detection of α-DG protein secreted into the cell culture media. The culture supernatant from cells cultured in the presence or absence of BB-2516 for 2 days was collected, and glycoproteins present in the medium were precipitated by wheat germ agglutinin-Sepharose. The precipitated proteins were subjected to immunoblot analysis using anti-α-DG antibody IIH6. A total cell extract from EpH4 cells was included as a positive control for α-DG expression and for molecular mass comparison.

(Lexington, KY). Secondary antibodies and anti-IgM-horseradish peroxidase (HRP) were purchased from Sigma (St. Louis, MO), and anti-immunoglobulin-HRP antibodies were from Amersham Pharmacia Biotech (Piscataway, NJ). Fluorescein isothiocyanate-conjugated secondary antibodies and streptavidin-HRP were from Caltag Laboratories (Burlingame, CA). Propidium iodide was purchased from Sigma. MP inhibitors BB-2516, GM6001, and control C1004 were purchased from AMS Scientific (Concord, CA). Furin inhibitor I [decanoyl-Arg-Val-Lys-Arg-chloromethyketone (CMK)] was purchased from Calbiochem (La Jolla, CA). MG-132 and brefeldin A were purchased from Sigma.

Cell Culture. The murine EpH4 cell line has been described previously (23). EpRas cells were obtained from Dr. Ernst Reichmann (Universitäts-Kinderspital Zürich, Zurich, Switzerland) and are a nonmalignant cell clone derived from Ras-transfected EpH4 cells (24). Human breast cancer cell lines MDA-MB-231, MDA-MB-468, T47D, and BT-474 were obtained from American Type Culture Collection (Manassas, VA). LoVo, LoVo-neo, LoVo-fur1, and LoVo-fur2 were kindly provided by Dr. Claire Dubois (University of Sherbrooke, Quebec, Quebec, Canada). LoVo cells transfected with furin were created in the laboratory of Dr N. Kitamura (Kansai Medical University, Osaka, Japan). LoVo cells were stably transfected with pCMVFur, a vector encoding wild-type furin cDNA, to create the clones LoVo-fur1 and LoVo-fur2 or transfected with a control vector pRC/CMV to create LoVo-neo (25).

All cell lines were cultured in Dulbecco's modified Eagle's medium:Ham's F-12 (Hyclone, Logan, UT). For EpH4 and EpRas cells, the medium was supplemented with 2% fetal bovine serum (FBS), 5 μg/ml insulin (Sigma) and 10 μg/ml gentamicin (Invitrogen, Carlsbad, CA). All of the cancer cell lines were cultured in medium supplemented with 5% FBS. LoVo cells and transfected derivatives were cultured in medium supplemented with 10% FBS. For serum starvation, cells were cultured in medium containing insulin and gentamicin for 2 to 3 days. Cells treated with protease inhibitors were cultured for 2 days in serum-free medium containing insulin (insulin and gentamicin for EpH4 and EpRas) and inhibitors before protein extraction. Inhibitor concentrations used were 5 μmol/L for BB-2516, 50 μmol/L for GM6001 and its control analog C1004, and 20 μmol/L for CMK.

Western Blots. Proteins were extracted from cells on plastic using cell lysis buffer [50 mmol/L Tris (pH 7.4), 1% (w/v) sodium deoxycholate, 1% (v/v) Nonidet P-40, 0.1% (w/v) SDS, and 150 mmol/L NaCl], and protease inhibitor mixture (Calbiochem). Insoluble material was removed by centrifugation at 12,000 × g for 15 minutes. Proteins were separated by standard SDS-PAGE using ready-made gels (Biowhittaker, Walkersville, MD) and transferred to Immobilion-P membranes (Millipore Corp., Billerica, MA). For

immunodetection of proteins, membranes were blocked in 5% nonfat dried milk in TBST buffer [20 mmol/L Tris (pH 7.5), 100 mmol/L NaCl, 0.1% (v/v) Tween 20] and then incubated with primary antibodies diluted in the blocking buffer. Membranes were washed four to five times in TBST buffer after incubation for 1 hour in secondary antibodies. Detection for the bound antibodies was done with either ECL-Plus (α- and β-DG) or enhanced chemiluminescence substrate (E-cadherin) according to the manufacturer's instructions (Amersham Pharmacia Biotech). Intensities of individual bands were quantified using a Fluorchem 8000 Chemi-Imager from Alpha Innotech (San Leandro, CA). When assessing the ratio of α-DG/β-DG, α- and β-DG levels were analyzed from the same transfer membranes to eliminate potential errors in protein loading. To achieve this, the transfer membranes were cut above the 50-kDa band, and the upper half was probed with anti-α-DG antibody, and the lower half was probed with anti-β-DG antibody. The band intensities of the 43- and 31-kDa isoforms of β-DG were summed to calculate the quantity of β-DG present. The laminin overlay assay was performed as described previously (16).

Immunofluorescence Staining. Cells were cultured in chamber slides and incubated with or without furin inhibitor for 2 days in serum-free medium. Cells were then washed twice with PBS, fixed with 2% paraformaldehyde in PBS for 10 minutes at room temperature, and washed again with PBS. Subsequently, cells were incubated in blocking buffer [PBS with 0.1% (v/v) Tween 20 and 10% goat serum] for 1 hour at room temperature and then incubated overnight with primary anti-α-DG antibody (IIH6) in blocking buffer at 4°C. Cells were then washed three times for 10 minutes each in PBS containing 0.1% (v/v) Tween 20. Cells were then incubated with secondary anti-IgM antibody conjugated to fluorescein isothiocyanate for 1 h at room temperature. The cells were counterstained for the nuclei with propidium iodide (10 μg/ml in PBS), washed, and then processed for fluorescence imaging.

Wheat Germ Agglutinin Precipitation. Culture supernatants of the cells cultured under various conditions were collected and concentrated 10 to 15 times using protein concentrator spin columns (Vivascience, Carlsbad, CA), and an equal amount of precipitation buffer [100 mmol/L Tris (pH 7.4), 300 mmol/L NaCl, and 1% Nonidet P-40] was added along with protease inhibitor mixture. Each sample was incubated with 50 μl of wheat germ agglutinin-agarose (Amersham Pharmacia Biotech) with rotation at 4°C overnight. The wheat germ agglutinin-agarose beads were washed three times with precipitation buffer and analyzed by SDS-PAGE and immunoblotting with anti-α-DG antibodies.

Biotinylation of Cell Surface Proteins and Coimmunoprecipitation. Cells cultured in 100-mm dishes were washed twice with ice-cold PBS and then incubated with 0.25 mg/ml of NHSPEO$_4$-biotin in PBS for 30 min at room temperature. Subsequently, cells were washed three times with PBS and then lysed in immunoprecipitation buffer [50 mmol/L Tris-HCl (pH 7.4), 100 mmol/L NaCl, 0.1% (v/v) Nonidet P-40, 1 mmol/L dithiothreitol, 1 mmol/L phenylmethylsulfonyl fluoride, and protease inhibitor mixture]. Cleared lysate was incubated with anti-β-DG monoclonal antibody overnight at 4°C, followed by the addition of protein A-agarose beads and a further incubation for 3 hours with continuous rotation at 4°C. The beads were subsequently washed three times with immunoprecipitation buffer and then resuspended in sample buffer directly, boiled, and processed for SDS-PAGE and immunoblotting for proteins conjugated with biotin using HRP-conjugated streptavidin.

Cleavage of α-Dystroglycan *In vitro* by Purified Furin. EpH4 cells were cultured in the presence of the furin inhibitor CMK for 2 days, and then cell surface proteins were biotinylated as described above. α-DG bound to β-DG was purified from the total cell extract by immunoprecipitation using anti-β-DG antibody as described above. DG complex bound to the protein A-agarose beads was directly incubated with pure furin (5–10U; Sigma) in digestion buffer [100 mmol/L HEPES (pH 7.6), 1 mmol/L CaCl$_2$, and 0.5% Triton X-100] for 2 h at 37°C. Subsequently, 4× SDS-PAGE sample buffer was directly added to the sample, and the sample was boiled and processed for immunoblotting with streptavidin, laminin, and anti-α-DG antibodies.

RESULTS

Metalloprotease Activity Induces α-Dystroglycan Shedding, Independent of β-Dystroglycan Cleavage. To investigate the regulation of DG composition in breast epithelial cells and carcinoma cells, we analyzed multiple cell lines with differing growth and tumorigenic properties. As reported previously (9), both α-DG and β-DG were detected in nontumorigenic mammary epithelial cells (*e.g.,* EpH4 and EpRas) and some nonaggressive breast cancer cell lines (*e.g.,* T47D and BT-474), although the ratio of α-DG/β-DG varied widely between these cell lines (ref. 9; Fig. 1*A* and *B*). In invasive tumor cell lines, such as MDA-MB-231 and MDA-MB-468, α-DG was undetectable using the IIH6 monoclonal antibody, but β-DG was still readily detected. The 31-kDa variant of β-DG was evident in all cell lines except BT-474 and EpH4 cells.

To investigate the role of proteases in the apparent loss of α-DG, we first tested the ability of MP inhibitors to alter the levels of α-DG in these cell lines and to increase the ratio of α-DG/β-DG. As shown in Fig. 1*B*, treatment with a general MP inhibitor (BB-2516) resulted in a substantial increase in α-DG levels in EpH4, EpRas, BT-474, and T47D cells. However, the MP inhibitor did not restore α-DG levels in cell lines originally lacking detectable levels of α-DG (MDA-MB-231 and MDA-MB-468; Fig. 1*B*). Likewise, serine protease, cysteine protease, and proprotein convertase (PC) inhibitors had no effect in restoring detectable α-DG to the MDA-MB-468 and MDA-MB-231 cell lines (data not shown).

As reported previously (22), MP inhibitor treatment caused the disappearance of the 31-kDa β-DG band in those cell lines that displayed this protein variant (Fig. 1*B*). Disappearance of the 31-kDa variant corresponded with increased levels of the full-length 43-kDa β-DG molecule, although this change was minor in all cell lines except EpRas. However, in those cell lines in which α-DG was detectable, α-DG levels were elevated to a greater extent than were the levels of β-DG by MP inhibitor treatment, effecting an increase in the ratio of α-DG/β-DG (Fig. 1*C*). Notably, EpH4 and BT-474 cells lacked any evidence of β-DG cleavage, yet the α-DG levels were elevated almost 2- and 3-fold, respectively, by the MP inhibitor. Together, these results demonstrated a MP-mediated mechanism for the loss of α-DG that was independent of β-DG cleavage by MPs. Another general MP inhibitor, GM6001, produced results similar to

those seen with BB-2516, and an inactive GM6001 analog (C1004) had no effect at the same concentrations (data not shown).

Loss of α-DG by MP activity could result either from direct cleavage of α-DG or indirectly, through, for example, cleavage of an associated protein, causing detachment of intact α-DG from the cell surface. To distinguish between these two possibilities, we examined the molecular mass of the shed α-DG in the culture medium by immunoblotting. α-DG was detected in the conditioned medium from the two cell lines we tested, and this shedding was almost completely inhibited in the presence of MP inhibitors (Fig. 1*D*). However, the molecular mass of the shed α-DG was comparable with that of the cell surface-bound form, indicating that α-DG itself may not be the target for MP-dependent shedding.
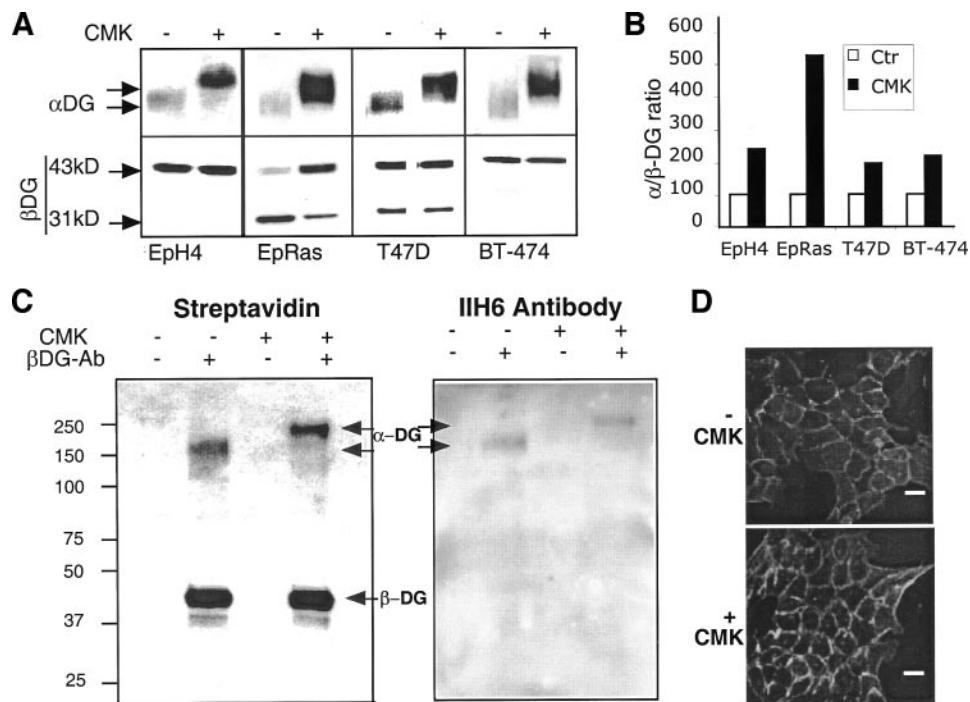
α-DG was not detected in conditioned medium from MDA-MB-468 and MDA-MB-231 cells (data not shown); therefore, the cause of the loss of α-DG detection in these cells was still unexplained. Likewise, α-DG was not detected in these cells after treatment with the trafficking inhibitor brefeldin A, which inhibits transport of molecules to the cell surface, or after treatment with the proteasome inhibitor MG132, which blocks protein degradation internally (data not shown). The proteasome inhibitor MG132 did specifically enhance the levels of the 31-kDa isoform of β-DG relative to the 43-kDa form, indicating that the 31-kDa cleavage product of β-DG is targeted for destruction in the proteasome (data not shown).

Proprotein Convertase Activity Facilitates α-Dystroglycan Shedding and Modifies α-Dystroglycan Composition. We next tested whether other proteases, in addition to MPs, participated in the regulation of α-DG shedding. Inhibitors of cysteine and serine proteases had no observable effect on α-DG shedding (data not shown). However, an inhibitor of the PCs, CMK, produced a dramatic effect on the levels and composition of the α-DG protein. Aside from an unexpected shift in molecular mass (investigated below), PC inhibition produced a substantial increase in α-DG levels (Fig. 2*A*) and a noticeable increase in the α-BG/β-DG ratio in all of the cell lines in which α-DG was detectable (Fig. 2*B*). In EpRas and T47D cells, cleavage of β-DG was only partially inhibited in the presence of CMK.

Surprisingly, not only were α-DG levels augmented by the inhibition of convertase activity, but the molecular mass of the α-DG molecule was also increased by approximately 40 kDa in all four cell lines (Fig. 2*A*). This upward shift in the molecular mass of α-DG was not caused by preventing cleavage of the full-length DG polypeptide into the α and β subunits because anti-β-DG antibodies did not detect the higher molecular mass ($\sim$190 kDa) form of α-DG (data not shown). In addition, there was no reduction in the levels of 43-kDa β-DG, despite the fact that the 150-kDa α-DG band completely disappeared in the cells treated with convertase inhibitor. We concluded, therefore, that convertase activity leads to posttranslational processing of α-DG through direct cleavage of α-DG into two molecules.

The two convertase cleavage products could both remain attached to the cell surface through noncovalent interactions, or one could be released as a soluble molecule. Lacking antibodies directed to both peptides, we resorted to a method of DG polypeptide detection that was independent of domain-specific antibodies. Extracellular proteins were labeled in living cells using cell surface biotinylation, and the DG complex present at the cell surface was then isolated by coimmunoprecipitation using the COOH-terminal β-DG antibody. Immunoprecipitated cell surface proteins were then detected using streptavidin-HRP. If both cleavage products remained firmly attached to β-DG, then both could be coprecipitated by this method and detected by streptavidin-HRP. Immunoprecipitation of the DG complex from EpH4 cells revealed a strong β-DG band at 43 kDa and a broad

Fig. 2. Evidence for PC-dependent cleavage of α-DG. *A*, effect of the PC inhibitor on the levels of α- and β-DG in normal mammary epithelial cells and breast tumor cell lines. Cells were cultured in serum-free medium for 2 days with or without the PC inhibitor CMK, and then total cellular proteins were extracted and subjected to immunoblot analysis of α-and β-DG. To eliminate potential errors in protein loading, α- and β-DG were analyzed from the same transfer membranes, which were cut above the 50-kDa band, and the upper half was probed with anti-α-DG antibody, and the lower half was probed with anti-β-DG antibody. *B*, α-DG/β-DG ratio levels in Fig. 2*A*. Intensities of bands were quantified, and the α-DG/β-DG ratio was calculated. The α-DG/β-DG ratio of untreated cells was set at 100%, and that of CMK treated cells was calculated as the percentage increase from the control. *C*, immunoprecipitation of β-DG-associated proteins in EpH4 cells. Cells were cultured in the presence or absence of CMK for 2 days, and then cell surface proteins were labeled with biotin. Proteins of the DG complex were immunoprecipitated using an anti-β-DG antibody and detected by either streptavidin-HRP binding to detect biotin-labeled cell surface proteins or immunoblotting with IIH6 antibody to detect α-DG. Immunoprecipitations lacking the primary antibody were used to control for nonspecific binding. *D*, localization of α-DG in the absence of PC-dependent cleavage. EpH4 cells were cultured for 2 days in the presence or absence of CMK and subjected to immunofluorescence staining to detect α-DG localization (*bar*, 20 μm).

secondary band at 150 kDa, corresponding to the molecular mass of α-DG, and a minor band was also observed at ~38 kDa (Fig. 2*C*). Immunoprecipitation of the DG complex from cells treated with the convertase inhibitor revealed a complete upward shift in the molecular mass of the 150-kDa band to about 190 kDa (Fig. 2*C*), matching the shift in α-DG detected when the IIH6 antibody was used (Fig. 2*A*). The inhibitor treatment did not alter the intensity of the 43-kDa β-DG band or alter the band at 38 kDa. Therefore, the second cleavage product (estimated at ~40 kDa) was not evident in these immuno-precipitations. Reprobing the same blot (after stripping the streptavi-din-HRP) with the IIH6 (anti-α-DG) antibody detected the 150- and 190-kDa bands (Fig. 2*C*). This result confirmed the coprecipitation of α-DG using the β-DG antibody, as expected, because the α-DG COOH-terminal domain directly associates with the β-DG NH₂-terminal domain (26). Therefore, we concluded that the ~40-kDa cleavage product, absent from the immunoprecipitations, comprises the NH₂-terminal portion of α-DG. Because the cleavage of α-DG by convertase activity was evident in all cell lines tested, this newly generated NH₂-terminal fragment represents a common and distinct molecule, and we refer to it here as "CN-DG" for cleaved NH₂-terminal α-DG.

The PCs might cleave DG within the Golgi and could affect transport to the cell surface. However, immunofluorescence staining of α-DG in EpH4 cells showed that α-DG stained prominently on the cell surface, with or without treatment with the convertase inhibitor CMK (Fig. 2*D*), indicating that lack of cleavage had no effect on transport of the DG molecule.
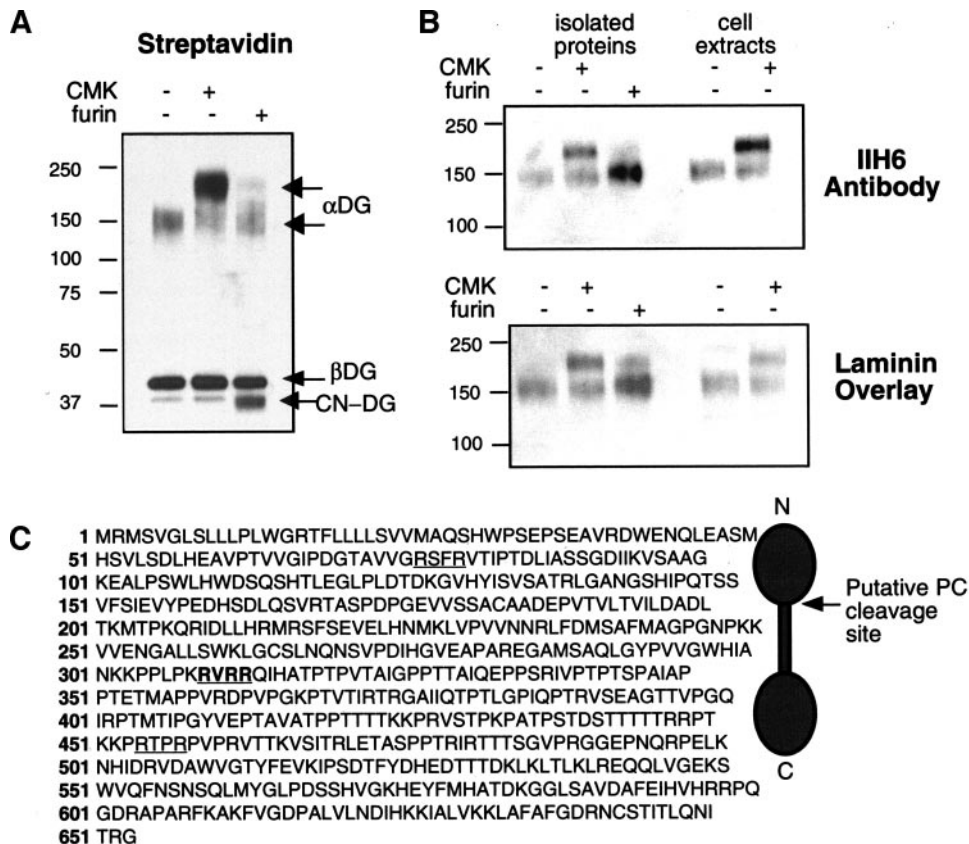
Furin Mediates Direct Cleavage of α-Dystroglycan. PCs are a family of more than six endopeptidases known to proteolytically activate a large number of proprotein substrates (27). In contrast to most PCs, which are expressed in a tissue-specific manner (28, 29), the PC furin is expressed in almost all tissues of the body. To ascertain whether furin could act directly on α-DG and to confirm that it did not act indirectly through a signaling cascade, we treated α-DG *in vitro* with purified furin to test for α-DG cleavage. For this experiment, we treated the EpH4 cells with or without CMK for 2 days and then biotinylated the cell surface proteins. Subsequently, full-length α- and

β-DG were immunoprecipitated using the anti-β-DG antibody and detected by streptavidin-HRP. Incubation of full-length α-DG with purified furin resulted in a reduction in the molecular mass of α-DG back to the original mass of 150 kDa and the creation of a new band at ~37 kDa that likely corresponds to the CN-DG molecule (Fig. 3*A*). Again, the immunoprecipitated α-DG was also detected using the IIH6 antibody on the same blot, after stripping of the streptavidin-HRP (Fig. 3*B*). Laminin overlay of the same membrane confirmed that the 150-kDa form of α-DG possessed the laminin-binding site (Fig. 3*B*). Probing of crude cell extracts (Fig. 3*B*) demonstrated the specificity the laminin overlay method. Therefore, both the laminin and IIH6 binding domains resided between this furin cleavage site, which defines the NH₂ terminus of α-DG, and the COOH terminus, which binds to β-DG.

Determination of the cleavage site in α-DG by direct peptide analysis of the α-DG NH₂ terminus has not yet been successful, apparently due to blockage of the NH₂ terminus. PCs cleave their substrates at the optimal consensus sequence of R-*X*-K/R-R ↓ [where *X* is any amino acid, and ↓ denotes the cleavage site (27)]. Survey of the α-DG peptide sequence identified only one optimal cleavage site (R-V-R-R) at amino acid 312, as shown in Fig. 3*B*, and this site is conserved from human to *Xenopus laevis*. Cleavage of α-DG at this site would remove a 312-amino acid–long polypeptide comprising the entire NH₂-terminal globular domain (Fig. 3*C*) and could account for the ~40-kDa loss in mass by the action of PCs.

Furin Cleavage in Living Cells. To determine whether the enzyme furin was indeed responsible for this cleavage in living cells, we obtained the invasive colon carcinoma cell line LoVo; this cell line is commonly used to assess furin functions because it lacks furin activity due to point mutations in both alleles (30). In addition, we obtained two independent clones of LoVo cells transfected with wild-type furin cDNA and designated LoVo-fur1 and LoVo-fur2 (25). To detect α-DG in LoVo cells without relying on epitope-specific antibodies, we chose to immunoprecipitate the DG complex from these cells after protein labeling by cell surface biotinylation, as described above (see Figs. 2*C* and 3*A*). Detection of the immunoprecipitated proteins in LoVo cells revealed the β-DG band at 43 kDa and a strong, broad

Fig. 3. Properties of α-DG fragments after direct cleavage by fuirn. *A*, direct cleavage of α-DG by furin. Full-length α- and β-DG were isolated by cell surface biotinylation and subsequent immunoprecipitation with β-DG antibody from EpH4 cells treated without (*Lane 1*) or with CMK (*Lanes 2* and *3*). The precipitated DG complex was then incubated with purified furin for 2 hours in the absence of furin inhibitor CMK (*Lane 3*). α-DG was detected by immunoblot using streptavidin-HRP. *B*, assays of IIH6 antibody and laminin binding to α-DG after furin cleavage. Full-length α- and β-DG were isolated by immunoprecipitation with β-DG antibody from EpH4 cells treated without (*Lane 1*) or with CMK (*Lanes 2* and *3*). The precipitated DG complex was then incubated with purified furin for 2 hours in the absence of furin inhibitor CMK (*Lane 3*). Total cell extracts of EpH4 cells treated without (*Lane 4*) and with CMK (*Lane 5*) were included to demonstrate the specificity of the laminin binding assay. *C*, complete amino acid sequence of human α-DG protein showing the location of potential PC cleavage sites. The one optimal cleavage site at amino acid 312 is *underlined* and *bold*, whereas minimal sites are *underlined*. The *diagram* on the *right* shows the dumbbell-shaped α-DG molecule along with the location of the optimal PC cleavage site right after the end of the NH₂-terminal globular domain.

band corresponding to α-DG at a molecular mass of 150 kDa (Fig. 4*A*). Significantly, in the LoVo cells expressing furin, the molecular mass of α-DG was reduced to slightly above 100 kDa (Fig. 4*A*). We confirmed that furin cleavage caused this reduction in the molecular mass by inhibiting this cleavage using the PC inhibitor CMK in furin-transfected LoVo cells, restoring the 150-kDa α-DG band seen in the parental LoVo cells (Fig. 4*B*).

The results in Fig. 4*B* indicate that LoVo cells expressed the full-length α-DG peptide; the α-DG COOH terminus was present and associated with the β-DG subunit, as evidenced by coimmunoprecipitation, and LoVo cells expressing furin possessed the NH₂ terminus of α-DG defined by the furin cleavage site. However, in LoVo cells expressing furin, α-DG migrated at little more than 100 kDa, approximately 50 kDa smaller than the α-DG detected in other cells lines (*e.g.,* EpH4, BT-474, and T47D). The smaller molecular mass form of α-DG observed in LoVo cells could be explained by hypoglycosylation of α-DG. Indeed, immunoblots for α- and β-DG expression showed that the form of α-DG expressed in LoVo cells was not detected by the IIH6 anti-α-DG monoclonal antibody or by laminin overlay (Fig. 4*C*; data not shown), both of which depend on proper glycosylation for epitope binding (15, 16).

Altered Glycosylation Is the Primary Cause of Loss of Dystroglycan Function in Invasive Carcinoma Cells. The lack of α-DG detection in LoVo cells by the IIH6 antibody and laminin was reminiscent of results obtained in other invasive carcinoma cell lines (ref. 9; Fig. 1). Therefore, we hypothesized that hypoglycosylation explained the absence of α-DG detection in invasive carcinoma cells such as MDA-MB-468 and MDA-MB-231 breast carcinoma cells. To test this hypothesis, the DG complex was immunoprecipitated from MDA-MB-468 and MDAMB-231 cells after cell surface biotinylation. Immunoprecipitations from these cells revealed the presence of a 43-kDa β-DG and a broad band corresponding to α-DG in both cell

lines (Fig. 5*A*). MDA-MB-468 and MDA-MB-231 cells both possess α-DG bands with a molecular mass of ~110 and 100 kDa, respectively, which was distinct from that of cells expressing functionally normal α-DG (*e.g.,* EpH4) but similar to that of LoVo cells expressing furin (Fig. 5*A*). Treatment of these cell lines with the CMK produced the expected increase in the molecular mass of α-DG (Fig. 5*A*); therefore, the NH₂ terminus of these proteins was defined by the furin cleavage site. Treatment of these cells with the MP inhibitor BB-2516 enhanced the levels of the 100–110-kDa bands (data not shown), indicating that MP-induced shedding of α-DG occurs in these cells, as it does in others (see Fig. 1*B*), yet MP inhibitors did not alter the molecular mass of the α-DG or restore α-DG detection by the IIH6 antibody (Fig. 1*B*). To directly test for laminin-1 binding in these carcinoma cells, we performed laminin overlay assays, using purified laminin-1. In contrast to normal cells, MDA-MB-468 and MDA-MB-231 cells did not bind laminin-1, demonstrating a loss of receptor function (Fig. 5*B*). Treatment of these cells with CMK or MP inhibitors did not recover laminin-1 binding activity (Fig. 5*B*; data not shown). Therefore, it was evident that α-DG is present in invasive breast carcinoma cells with the polypeptide sequence extending from the NH₂ terminus, defined by the furin cleavage site, to the COOH terminus. However, the fully processed α-DG protein is displayed at a smaller molecular mass due to hypoglycosylation, which also causes a loss of the IIH6 binding epitope and laminin binding.

DISCUSSION

The results presented here reveal several novel events of posttranslational processing that regulate DG function in normal epithelial cells and carcinoma cells. The results reveal that furin directly cleaves α-DG, changing our perception of the composition of α-DG and uncovering potentially important aspects of function and regulation in
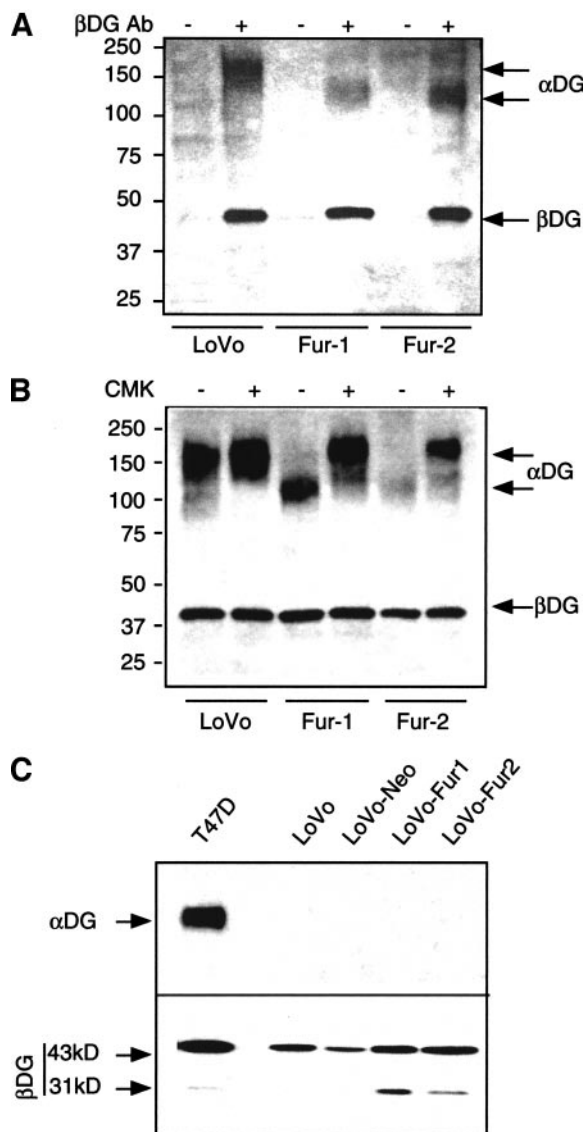
Fig. 4. Detection of dystroglycan isoforms in LoVo cells. *A*, immunoprecipitation of the DG complex from LoVo cells and furin-transfected derivatives. Cell surface proteins were labeled with biotin. Proteins of the DG complex were immunoprecipitated using an anti-β-DG antibody and detected by streptavidin-HRP binding to detect biotin-labeled cell surface proteins. Immunoprecipitations lacking the primary antibody were used to control for nonspecific binding. *B*, immunoprecipitation of the DG complex from LoVo cells and furin-transfected derivatives in the presence of the furin inhibitor CMK. Cells were cultured in the presence or absence of CMK for 2 days. Cell surface proteins were labeled with biotin. Proteins of the DG complex were immunoprecipitated using an anti-β-DG antibody and detected by streptavidin-HRP binding to detect biotin-labeled cell surface proteins. *C*, immunoblot analysis of total cellular extracts from LoVo cells and furin-transfected derivatives (LoVo-fur1 and LoVo-fur2) together with T47D cell extract as a positive control for α-and β-DG detection. Cells were grown in the presence of serum, equal amounts of proteins were loaded in each lane, and the transfer membrane was cut, as described in the text, to detect α- and β-DG separately, from the same membrane.

the DG molecule. We provide insights into the mechanism of α-DG shedding through the action of proteases, demonstrating new roles for MPs and furin. Importantly, we show that altered glycosylation is the primary cause for deficiencies in α-DG that occur in invasive cancer cells, revealing novel molecular defects that accompany cancer progression.

Direct Processing of Dystroglycan by Furin. One of the most surprising observations presented here is the previously unrecognized fact that α-DG can be processed by the PC furin into two molecules. PCs are known to activate molecules through removal of a propeptide (27). Observing such a cleavage in DG suggests that DG function too is altered or regulated through removal of an NH₂-terminal peptide.

Cleavage of α-DG by furin creates distinct molecules, warranting distinct names to designate them. The major fragment (~150 kDa in EpH4 cells) associates with β-DG, as determined by coimmunoprecipitation, and retains the laminin-binding epitope, as determined by laminin overlay (ref. 9; Fig. 5*B*). Therefore, the 150-kDa molecule corresponds to the mucin-like domain and a COOH-terminal globular domain, where the associations with laminin and β-DG, respectively, have been mapped (16, 26). This molecule is also detected by the IIH6 and VIA4 antibodies (9, 20), which have been widely used to define α-DG expression and localization. For this reason, we propose that the 150-kDa molecule retain the designation α-DG. We now designate as CN-DG (for cleaved NH₂-terminal α-DG) the 37-kDa cleavage product that corresponds to what was previously considered the NH₂-terminal portion of α-DG.
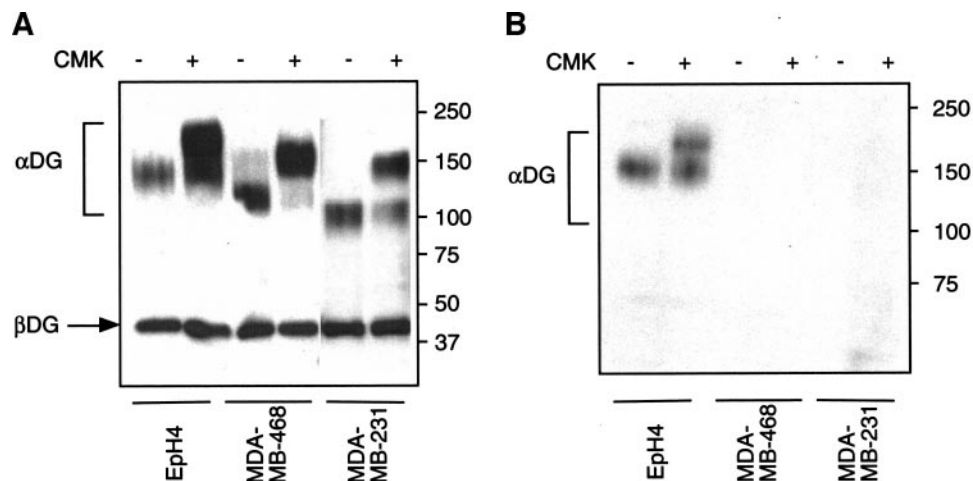
Although not directly confirmed by protein sequence analysis, all evidence indicates that the furin cleavage site occurs at amino acid 312. Only this one site in the α-DG amino acid sequence matches the optimal sequence for furin cleavage (R-*X*-K/R-R). The observed shift in molecular mass of about ~40 kDa coincides with the estimated mass of the 312-amino acid–long polypeptide (~34 kDa), plus added carbohydrates. This predicted mass was even more closely approximated by the CN-DG band, which was detected at 37 kDa after *in vitro* furin cleavage (Fig. 3*A*).

All epithelial cell lines tested, whether normal or malignant, displayed complete processing of α-DG by furin (with the exception of furin-deficient LoVo cells). It remains to be determined how commonly this cleavage event occurs *in vivo* and to what extent this cleavage regulates DG functions. Furin expression is nearly ubiquitous *in vivo* (28), suggesting that cleavage of α-DG by furin might be widespread.

Currently, the functional significance of this furin-mediated cleavage is unknown. The cleaved α-DG, like the full-length α-DG, retains the ability to interact with laminin, as shown by laminin overlay (Figs. 3 and 5). The NH₂-terminal globular domain of α-DG has some homology with immunoglobulins (31) and was previously shown to be required for binding to viruses (32). Therefore cleavage of this domain may serve as a defense against infections. Of particular interest is the question of whether CN-DG remains associated with α-DG or is released as a soluble molecule. At present, immunoprecipitations of the DG complex from EpH4 cells, LoVo cells, and breast tumor cell lines (Figs. 2–5) have not detected evidence of CN-DG association at the cell surface. The fate of CN-DG *in vivo* is not known, but, intriguingly, if CN-DG is secreted, then it may possess unique functions that have yet to be explored.

Factors Involved in α-Dystroglycan Shedding. Our results have confirmed reports that β-DG cleavage at the cell surface is blocked by MP inhibitors (22). However, contrary to previous conclusions, we find that cleavage of β-DG is not the primary mechanism for loss of α-DG because MP inhibitors increase the overall α-DG/β-DG ratio and increase the levels of α-DG even in cells in which β-DG cleavage is not evident (EpH4 and BT-474 cells). Therefore, release of α-DG from the cell surface is clearly independent of β-DG cleavage. Shedding of α-DG could occur through cleavage of α-DG itself or through cleavage of some associated protein in the DG complex. However, in the cells tested here, we observed no reduction in the molecular mass of shed α-DG, implying that α-DG shedding might be a secondary event subsequent to the cleavage of an associated protein. In support of this model, the loss of α-sarcoglycan or δ-sarcoglycan, both of which are DG-associated molecules, is known to destabilize α-DG attachment to the cell surface in muscle cells (33, 34). Although most DG-associated proteins have not yet been observed in epithelial cells (35), immunoprecipitations of the DG complex did reveal a band at 38 kDa (Figs. 2 and 3), suggesting their presence. However, the 38-kDa

Fig. 5. Altered processing of α-DG and loss of DG function in invasive breast cancer cell lines. *A*, immunoprecipitation of the DG complex from EpH4, MDA-MB-231, and MDA-MB-468 cells revealed bands corresponding to α-DG at 150 kDa in normal cells and 100 kDa in carcinoma cells. The bands were shifted upward to about 150 kDa in the invasive carcinoma cells after treatment with CMK for 2 days. *B*, laminin binding in carcinoma cells. Proteins from *A* were assayed for laminin binding by laminin overlay. Laminin binding was detected in EpH4 control cells, but not in MDA-MB-231 and MDA-MB-468 cells, with or without treatment with the PC inhibitor CMK.

protein band has not been observed to change in the presence of protease inhibitors, and the precise mechanism of α-DG shedding remains obscure.

Inhibition of PCs also blocked α-DG shedding, as revealed by the marked increase in α-DG/β-DG ratio in all cell lines tested. The mechanism for this is unknown, but it may result from furin-dependent activation of the MP(s) responsible for α-DG shedding. Alternatively, the processing of α-DG by furin may render α-DG more susceptible to shedding through another mechanism. Significantly, both MPs and furin have been implicated in cancer progression (36, 37), and their ability to induce α-DG shedding may contribute to their cancer-promoting properties.

Of course, it remains to be determined how commonly α-DG shedding occurs *in vivo* and to what extent this shedding regulates DG functions. The significance of β-DG cleavage is also in question. It is

possible that cleavage of β-DG is secondary to α-DG shedding, in which release of α-DG from the cell surface exposes the 43-kDa β-DG to cleavage by MPs and its subsequent degradation. It appears that cleavage of β-DG directs the 31-kDa form to the proteasome for degradation, suggesting this cleavage is a signal for turnover of the protein.

Loss of α-Dystroglycan in Invasive Carcinoma Cells. Several reports have shown that DG function is frequently compromised in carcinoma cells, including cells from breast and colon cancers (9, 20, 21). However, none of the studies have revealed the mechanism for this DG deficiency, except for the suggestion that β-DG cleavage leads to loss of α-DG from the cell surface. Here we show clear evidence that although it appears that α-DG can be shed from the surface of all cells, altered glycosylation is the primary cause for loss of α-DG detection and loss of α-DG binding to ECM molecules in
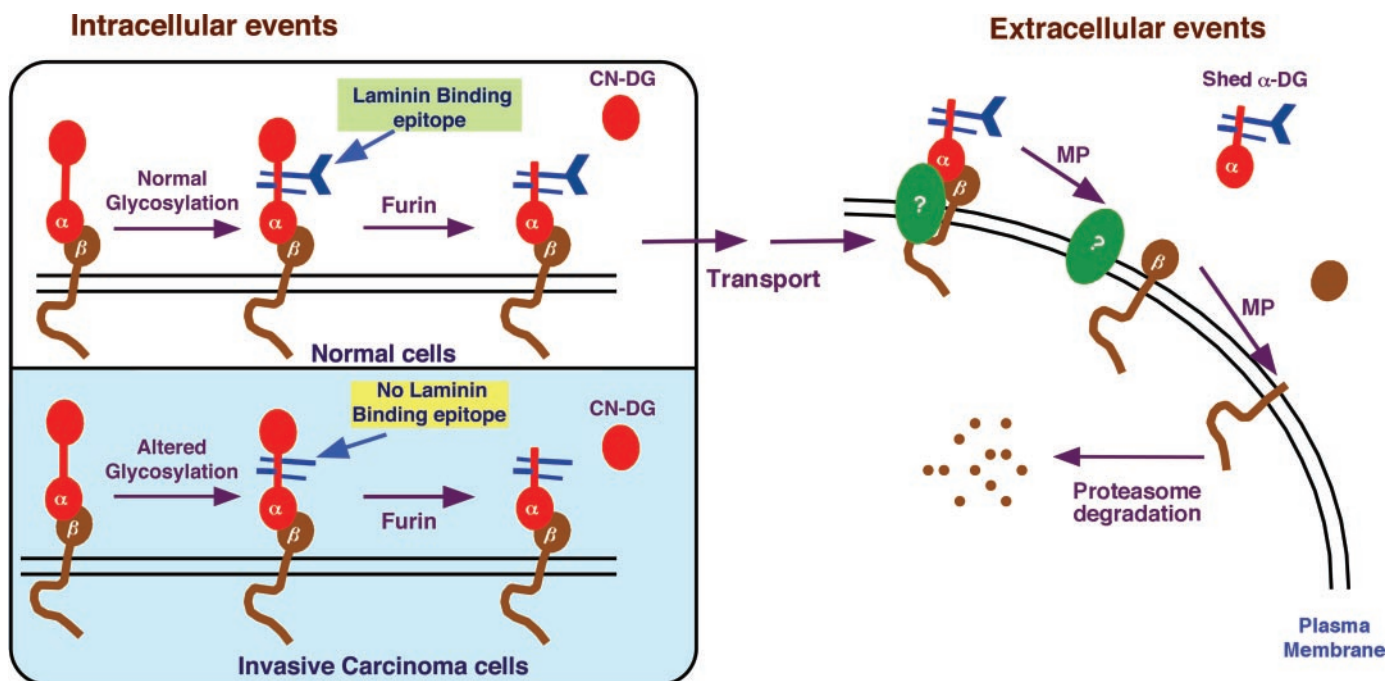

Fig. 6. Hypothetical model of the processing events modulating α-DG function. In normal cells and noninvasive carcinoma cells, the glycosylation of α-DG takes place in the Golgi, creating a functional laminin-binding epitope. In addition, furin cleaves α-DG to release the CN-DG molecule. The mature α-DG/β-DG dimer assembles with unknown DG-associated molecules (*green oval molecule*) in the membrane. At the cell surface, MP-dependent cleavage of a DG-associated protein(s) leads to dissociation of the dystroglycan complex, resulting in the shedding of α-DG from the cell surface. This in turn renders the 43-kDa β-DG molecule susceptible to MP-dependent cleavage to form a 31-kDa variant that is internalized and degraded through the proteasome pathway. These same events occur in invasive carcinoma cells, except that initial glycosylation steps are defective, resulting in a completely nonfunctional α-DG (*i.e.*, one that is unable to bind to basement membrane components).

invasive carcinoma cells. Immunoprecipitations of the DG complex revealed an abnormally small (~100–110-kDa) form of α-DG in invasive carcinoma cell lines (MDA-MB-231, MDA-MB-468, and LoVo cells expressing furin), despite the fact that they express a polypeptide with the NH_2 terminus defined by the furin cleavage site. This form was not detected by the carbohydrate-dependent IIH6 antibody or by laminin overlay, demonstrating altered glycosylation and loss of receptor function. MP and PC inhibitors failed to restore α-DG detection using the IIH6 antibody or to restore laminin binding in these cells. Altered glycosylation explains all of these observations and explains why overexpression of DG cDNA failed to enhance α-DG detection or function in the same breast cancer cell lines (9). There are a growing number of reports on the role of altered glycosylation of α-DG in diseases, including muscular dystrophies and neurodegenerative diseases (13, 17). To our knowledge, this is the first report showing that altered α-DG glycosylation contributes to the functional modulation of DG in cancer cells, possibly adding invasive cancer to the list of "dystroglycanopathies" (13).

Our results provide a new schematic for the modulation of DG in normal and carcinoma cells and point to several mechanisms for the regulation of DG that can be exploited to enhance or restore DG function. We provide a working model of these events in Fig. 6. Although results in this study have been limited to epithelial cells, it is possible that MPs and/or PCs also promote the loss of α-DG in some muscular dystrophies. It will now be important to determine the precise cause of α-DG shedding, the nature of carbohydrate alterations in cancer cells, and what factors regulate these events. Understanding the regulation of DG is critical to discern mechanisms of normal development and disease progression and may aid in the discovery of new therapies for many diseases including muscular dystrophies and cancer.

ACKNOWLEDGMENTS

REFERENCES

1. Henry MD, Campbell KP. Dystroglycan inside and out. Curr Opin Cell Biol 1999; 11:602–7.
2. Weir ML, Muschler J. Dystroglycan: emerging roles in mammary gland function. J Mammary Gland Biol Neoplasia 2003;8:409–19.
3. Ervasti JM, Campbell KP. Membrane organization of the dystrophinglycoprotein complex. Cell 1991;66:1121–31.
4. Ervasti JM, Campbell KP. A role for the dystrophin-glycoprotein complex as a transmembrane linker between laminin and actin. J Cell Biol 1993;122:809–23.
5. Cohn RD, Henry MD, Michele DE, et al. Disruption of DAG1 in differentiated skeletal muscle reveals a role for dystroglycan in muscle regeneration. Cell 2002; 110:639–48.
6. Moore SA, Saito F, Chen J, et al. Deletion of brain dystroglycan recapitulates aspects of congenital muscular dystrophy. Nature (Lond) 2002;418:422–5.
7. Henry MD, Campbell KP. A role for dystroglycan in basement membrane assembly. Cell 1998;95:859–70.
8. Durbeej M, Larsson E, Ibraghimov BO, et al. Non-muscle alpha-dystroglycan is involved in epithelial development. J Cell Biol 1995;130:79–91.
9. Muschler J, Levy D, Boudreau R, et al. A role for dystroglycan in epithelial polarization: loss of function in breast tumor cells. Cancer Res 2002;62:7102–9.
10. Deng WM, Schneider M, Frock R, et al. Dystroglycan is required for polarizing the epithelial cells and the oocyte in Drosophila. Development (Camb) 2003;130:173–84.
11. Rambukkana A, Yamada H, Zanazzi G, et al. Role of alpha-dystroglycan as a Schwann cell receptor for Mycobacterium leprae. Science (Wash DC) 1998;282: 2076–9.
12. Cao W, Henry MD, Borrow P, et al. Identification of alpha-dystroglycan as a receptor for lymphocytic choriomeningitis virus and Lassa fever virus. Science (Wash DC) 1998;282:2079–81.
13. Michele DE, Campbell KP. Dystrophin-glycoprotein complex: post-translational processing and dystroglycan function. J Biol Chem 2003;278:15457–60.
14. Henry MD, Cohen MB, Campbell KP. Reduced expression of dystroglycan in breast and prostate cancer. Hum Pathol 2001;32:791–5.
15. Chiba A, Matsumura K, Yamada H, et al. Structures of sialylated O-linked oligosaccharides of bovine peripheral nerve alpha-dystroglycan. The role of a novel O-mannosyl-type oligosaccharide in the binding of alpha-dystroglycan with laminin. J Biol Chem 1997;272:2156–62.
16. Michele DE, Barresi R, Kanagawa M, et al. Post-translational disruption of dystroglycan-ligand interactions in congenital muscular dystrophies. Nature (Lond) 2002; 418:417–22.
17. Muntoni F, Brockington M, Torelli S, Brown SC. Defective glycosylation in congenital muscular dystrophies. Curr Opin Neurol 2004;17:205–9.
18. Matsumura K, Chiba A, Yamada H, et al. A role of dystroglycan in schwannoma cell adhesion to laminin. J Biol Chem 1997;272:13904–10.
19. Shimizu H, Hosokawa H, Ninomiya H, Miner JH, Masaki T. Adhesion of cultured bovine aortic endothelial cells to laminin-1 mediated by dystroglycan. J Biol Chem 1999;274:11995–12000.
20. Losasso C, Di Tommaso F, Sgambato A, et al. Anomalous dystroglycan in carcinoma cell lines. FEBS Lett 2000;484:194–8.
21. Sgambato A, Migaldi M, Montanari M, et al. Dystroglycan expression is frequently reduced in human breast and colon cancers and is associated with tumor progression. Am J Pathol 2003;162:849–60.
22. Yamada H, Saito F, Fukuta-Ohi H, et al. Processing of beta-dystroglycan by matrix metalloproteinase disrupts the link between the extracellular matrix and cell membrane via the dystroglycan complex. Hum Mol Genet 2001;10:1563–9.
23. Reichmann E, Ball R, Groner B, Friis RR. New mammary epithelial and fibroblastic cell clones in coculture form structures competent to differentiate functionally. J Cell Biol 1989;108:1127–38.
24. Oft M, Peli J, Rudaz C, et al. TGF-beta1 and Ha-Ras collaborate in modulating the phenotypic plasticity and invasiveness of epithelial tumor cells. Genes Dev 1996;10: 2462–77.
25. Komada M, Hatsuzawa K, Shibamoto S, et al. Proteolytic processing of the hepatocyte growth factor/scatter factor receptor by furin. FEBS Lett 1993;328:25–9.
26. Bozzi M, Veglia G, Paci M, et al. A synthetic peptide corresponding to the 550–585 region of alpha-dystroglycan binds beta-dystroglycan as revealed by NMR spectroscopy. FEBS Lett 2001;499:210–4.
27. Thomas G. Furin at the cutting edge: from protein traffic to embryogenesis and disease. Nat Rev Mol Cell Biol 2002;3:753–66.
28. Dubois CM, Blanchette F, Laprise MH, et al. Evidence that furin is an authentic transforming growth factor-beta1-converting enzyme. Am J Pathol 2001;158:305–16.
29. Durbeej M, Henry MD, Ferletta M, Campbell KP, Ekblom P. Distribution of dystroglycan in normal adult mouse tissues. J Histochem Cytochem 1998;46:449–57.
30. Takahashi S, Nakagawa T, Kasai K, et al. A second mutant allele of furin in the processing-incompetent cell line, LoVo. Evidence for involvement of the homo B domain in autocatalytic activation. J Biol Chem 1995;270:26565–9.
31. Bozic D, Engel J, Brancaccio A. Sequence analysis suggests the presence of an IG-like domain in the N-terminal region of alpha-dystroglycan which was crystallized after mutation of a protease susceptible site (Arg168→His). Matrix Biol 1998;17: 495–500.
32. Kunz S, Sevilla N, McGavern DB, Campbell KP, Oldstone MB. Molecular analysis of the interaction of LCMV with its cellular receptor [alpha]-dystroglycan. J Cell Biol 2001;155:301–10.
33. Duclos F, Straub V, Moore SA, et al. Progressive muscular dystrophy in alpha-sarcoglycan-deficient mice. J Cell Biol 1998;142:1461–71.
34. Holt KH, Crosbie RH, Venzke DP, Campbell KP. Biosynthesis of dystroglycan: processing of a precursor propeptide. FEBS Lett 2000;468:79–83.
35. Durbeej M, Campbell KP. Biochemical characterization of the epithelial dystroglycan complex. J Biol Chem 1999;274:26609–16.
36. Bassi DE, Mahloogi H, Lopez De Cicco R, Klein-Szanto A. Increased furin activity enhances the malignant phenotype of human head and neck cancer cells. Am J Pathol 2003;162:439–47.
37. Egeblad M, Werb Z. New functions for the matrix metalloproteinases in cancer progression. Nat Rev Cancer 2002;2:161–74.